

Vibrational Spectroscopic Investigation of the Phase Diagram of a Biomimetic Lipid Monolayer

Sylvie Roke,¹ Juleon Schins,^{2,†} Michiel Müller,² and Mischa Bonn^{1,*}

¹*Leiden Institute of Chemistry, P.O. Box 9502, 2300 RA Leiden, The Netherlands*

²*Swammerdam Institute for Life Sciences, University of Amsterdam, P.O. Box 94062, 1090 GB Amsterdam, The Netherlands*

(Received 5 September 2002; published 26 March 2003)

The phase behavior of a biomimetic monolayer consisting of diphospholipid molecules on water is investigated using vibrational sum-frequency generation and fluorescence microscopy. In addition to the transition from the — molecularly disordered — liquid phase to the highly ordered and oriented condensed phase, a novel, extremely sharp transition is observed at low compression, which is attributed to the uncurling of the hydrophobic alkane chains upon compression.

DOI: 10.1103/PhysRevLett.90.128101

PACS numbers: 87.16.Dg, 42.65.-k, 68.37.-d, 68.60.-p

The interest in the behavior of phospholipid layers on water is due to its importance as a key constituent of biological membranes. Lipid molecules, such as L-1,2-Dipalmitoyl-*sn*-glycero-3-phosphocholine (DPPC) under study here, consist of a polar headgroup and two long apolar alkyl chains, as shown in the inset of Fig. 1. This structure gives rise to fascinating behavior, such as self-organization into different phases [2]. Monolayers are excellent model systems for membrane biophysics, since a biological membrane can be considered as two weakly coupled monolayers [2]. Of particular interest is the phase behavior as a function of lateral pressure, which has been studied with various thermodynamic and spectroscopic techniques [2]. It is clear that insights into the molecular and mesoscopic structure associated with the phase behavior of phospholipid layers are essential for a complete understanding of cell membrane and vesicle properties.

We have investigated the phase behavior of a DPPC monolayer on water using vibrational sum-frequency spectroscopy [3] (VSFG) in conjunction with fluorescence microscopy [1]. Second-order nonlinear spectroscopies with their intrinsic surface sensitivity [3] have provided important molecular-level insights into biological surface systems [4]. In particular, VSFG [5] has been used to probe DPPC phospholipid layers at the liquid-liquid interface as well as the kinetics of bilayer formation from vesicle rupture [6] by monitoring C—H stretch vibrations of both CH₂ and terminal CH₃ groups in the alkyl chain. VSFG is a very powerful spatially averaged local probe of molecular structure and orientation and provides information that is complementary to that obtained with the spatially resolved, but molecularly unspecific, fluorescence microscopy [1].

Using VSFG we observe, for the first time, a very sharp transition from a phase with curled alkyl chains to a phase with spatially extended chains. This transition, occurring at relatively low DPPC densities, cannot be observed with fluorescence microscopy and is not accompanied by significant changes in surface pressure. In addition, we analyze the order and orientation of the alkyl chains throughout the phase diagram.

DPPC was obtained from Avanti Polar Lipids (Birmingham, Alabama), as was the fluorescent probe, 1-palmitoyl-2-[12-[(7-nitro-2,1,3-benzoxadiazol-4-yl)-amino]dodecanoyl]-*sn*-glycero-3-phosphocholine (NBD-PC). The fluorescence experiments were carried out with a probe concentration of 0.5 mol % [1]. The phospholipid was spread from a chloroform solution (Fisher HPLC grade) of 1 mM concentration onto Millipore water (18.2 MΩ cm resistivity) of pH 7, in a homebuilt Teflon trough [dimensions (6 × 40) cm²]. Fluorescence images were taken with a charge-coupled device (CCD) camera mounted on a fluorescence microscope, with a 20 × /0.4 NA achromat microscope objective. The VSFG experiments (without fluorescent probe) were performed using 120 fs (6 μJ) infrared pulses (FWHM bandwidth of ~180 cm⁻¹) centered at 2930 cm⁻¹ and 3.5 μJ, 800 nm pulses with an 11 cm⁻¹ bandwidth, unless otherwise

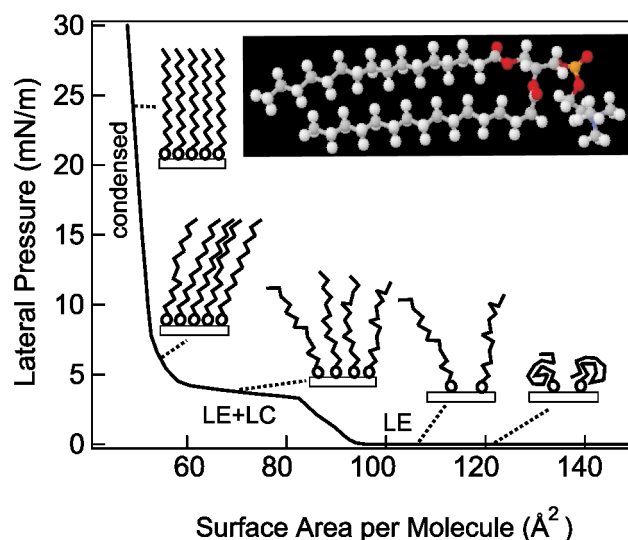


FIG. 1 (color online). Phase diagram of DPPC showing the condensed, liquid compressed–liquid expanded coexistence and the liquid expanded phase. After Refs. [1]. Also shown in the inset is a molecular model of DPPC. Schematic drawings of the lipid monolayer illustrate the main findings in this work.

specified (repetition rate 1 kHz). Spectra are obtained by dispersing the VSGF light onto a CCD camera [7], and averaging for typically 200 s. The pulses, focused down to a ~ 0.4 mm beamwaist, are incident at a 65° angle with respect to the surface normal.

Figure 1 depicts the lateral pressure of a DPPC monolayer as a function of surface area per molecule, known to reflect the existence of several phases [1,2]: a condensed phase at high compression (molecular area $A < 47 \text{ \AA}^2/\text{molecule}$), a liquid condensed (LC) phase, coexisting with the liquid expanded (LE) phase between 50 and $80 \text{ \AA}^2/\text{molecule}$, and the LE phase for $A > 80 \text{ \AA}^2/\text{molecule}$. At much higher surface areas ($A \geq 400 \text{ \AA}^2/\text{molecule}$), there exists an additional gas (G) phase [2].

Figure 2 depicts three sets of spectra at different polarization combinations (s or p) of the SFG, VIS, and IR light, respectively, indicated in the graph: for the compressed layer (top, $47 \text{ \AA}^2/\text{molecule}$), in the decompression region (middle, $58 \text{ \AA}^2/\text{molecule}$), and in the coexistence region (bottom, $65 \text{ \AA}^2/\text{molecule}$). The absence of signal for other polarization combinations (apart from pss , identical to sps) establishes that the surface is isotropic around its azimuth [8]. The fluorescence microscopy images (Fig. 2) reveal the onset of domain formation at $\sim 80 \text{ \AA}^2/\text{molecule}$ (not shown in the figure). These domains grow increasingly dense with further compression, in good agreement with previous observations [1].

The VSGF spectra $I_{\text{SFG}}(\omega)$ can be reproduced very well by an expression for the second-order nonlinear susceptibility consisting of a nonresonant term $\chi_{\text{NR}}^{(2)}$ and a resonant term $\chi_{\text{R}}^{(2)}$ associated with the vibrational transition, convoluted (\otimes) with the VIS up-conversion field obtained from its intensity [9]:

$$I_{\text{SFG}}(\omega) \propto |E_{\text{VIS}}(\omega) \otimes \chi^{(2)}(\omega_{\text{IR}})|^2;$$

$$\chi^{(2)} = \chi_{\text{NR}}^{(2)} + \chi_{\text{R}}^{(2)}$$

$$= A_0 e^{i\phi} + \sum_n \frac{A_n}{\omega_{\text{IR}} - \omega_n + i\Gamma_n}, \quad (1)$$

where the vibrational resonances are described by their resonance frequencies ω_n , linewidths $2\Gamma_n$, and amplitudes A_n . A_0 is the amplitude of the nonresonant susceptibility and ϕ its phase relative to the vibrational resonances.

For the strongly compressed DPPC layer ($47 \text{ \AA}^2/\text{molecule}$), the three spectra require three resonances, well-established for terminal CH_3 groups: the symmetric stretch at 2878 cm^{-1} , the asymmetric stretch at 2963 cm^{-1} , and a Fermi resonance at 2938 cm^{-1} . As VSGF is inherently sensitive only to media lacking inversion symmetry [3], CH_2 resonances (at ~ 2850 and $\sim 2920 \text{ cm}^{-1}$) are absent for a layer with all-trans alkyl chains, since these possess such symmetry [5,6,10]. Indeed, upon decompression of the layer to $58 \text{ \AA}^2/\text{molecule}$, the two CH_2 resonances associated with

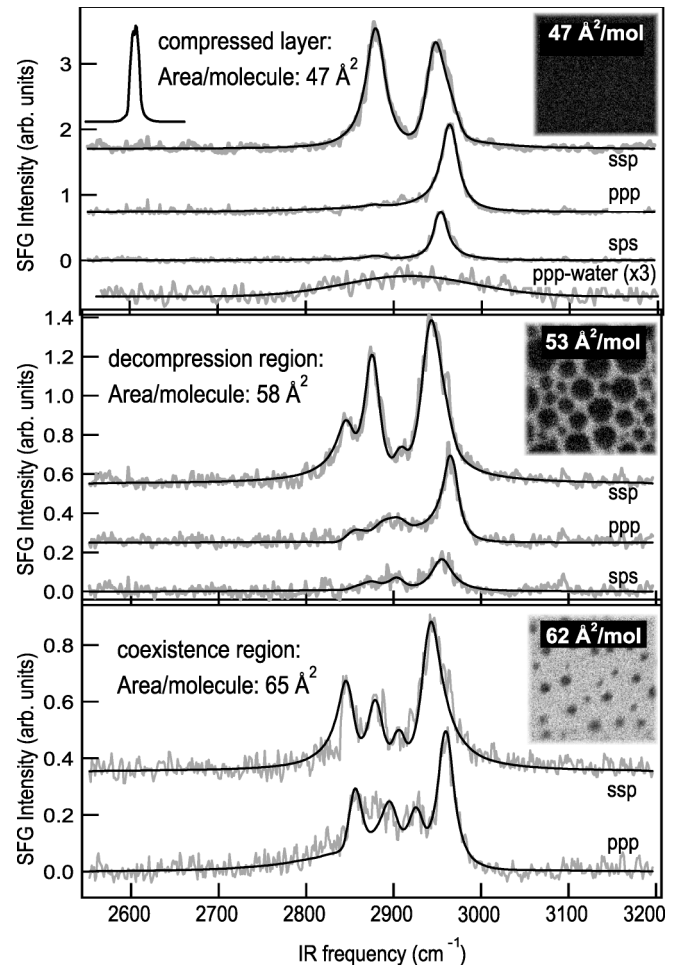


FIG. 2. SFG spectra (gray lines) obtained at different polarization conditions (the three letter code next to the spectra indicates polarizations for VSGF, VIS, and IR, respectively), in combination with fluorescence microscopy images ($50 \mu\text{m} \times 50 \mu\text{m}$) at various stages of compression (no structure for full compression). Black lines are fits described in the text. The spectral profile of the VIS up-conversion pulse is depicted in the upper left corner of the upper panel, which also depicts the signal from a bare water surface for ppp combination, reflecting the IR pulse bandwidth.

gauche defects appear: The alkyl chain is no longer perfectly stretched, as demonstrated previously [10]. Further decompression to $65 \text{ \AA}^2/\text{molecule}$ results in a further increase of these CH_2 modes, as well as a marked decrease in the CH_3 intensity, both testimony of disorder in the monolayer. The experimental spectra are fitted under the global constraint of fixed frequencies for the transitions, with linewidths varying in the range $\Gamma = 4.5\text{--}7 \text{ cm}^{-1}$. This constraint results in ineffectual fits for $65 \text{ \AA}^2/\text{molecule}$ (lower panel of Fig. 2), since it does not allow for different types of DPPC domains, from which the signals may interfere.

For a fully stretched (all-trans) DPPC molecule, as depicted in Fig. 1, the transition dipole moment of the

two CH_3 symmetric stretch vibrations (which lie along the terminal C—C bond in the alkyl chain) make an angle of $\sim 38^\circ$ and $\sim 45^\circ$ with the molecular axis (defined here along the lower of the two alkyl chains in Fig. 1). Neglecting this small angular difference and treating the DPPC molecule as two uncorrelated alkyl chains, we can deduce the orientation of the chains, by comparing the amplitude of the $\chi_{\alpha\beta\gamma}^{(2)}$ ($\alpha, \beta, \gamma = s$ or p) of the CH_3 C—H stretching mode for the different polarization combinations, as described in detail in Ref. [8]. For the required Fresnel coefficients, the complex refractive indices in air (n_1), water (n_2), and the interface layer (n'_1) for the three beams are set as $n_1 = 1$ and $n'_1 = 1.18$ [8] for all beams; $n_2^{\text{IR}} = 1.39 + 0.013i$; $n_2^{\text{VIS}} = 1.326 + 1.3 \times 10^{-7}i$ and $n_2^{\text{SFG}} = 1.331$. For the fully compressed phase ($47 \text{ \AA}^2/\text{molecule}$), the molecular axis lies along the surface normal, tilting to an angle of $\sim 20^\circ$ in the decompression region ($58 \text{ \AA}^2/\text{molecule}$).

Compressing the layer, Fig. 3 demonstrates that, starting at very low densities ($A \geq 110 \text{ \AA}^2/\text{molecule}$), no signal is observed in the C—H stretch region, despite the fact that some nonresonant VSGF is generated at the surface. Further compression of the layer leads to the sudden appearance of two resonances around 2850 and 2920 cm^{-1} , associated mainly with CH_2 moieties in the disordered alkyl chain (although some contribution from the CH_3 groups cannot be excluded; to obtain sufficient signal-to-noise the spectral resolution in this set of experiments is 40 cm^{-1}).

These two peaks can be reproducibly (and without significant hysteresis) “switched on and off” by very slight recompression and decompression, where the system must be allowed to equilibrate for some 20 sec. Note that the change in surface coverage between the presence and the absence of the signal is less than 1%. The numbers next to the spectra (in parentheses) denote the order in which the spectra were recorded in this particular run. There is a surprisingly sharp and sudden change in the signal (also observed under ppp -polarization conditions) as a function of molecular surface area. This transition is not caused by laser effects: Variation of the pulse energies and laser repetition rate over 1 order of magnitude and beam focus sizes over a factor of 2 does not affect the presence of the transition. We did observe a slight shift in the exact position of the transition, converging to a value of $115 \pm 3 \text{ \AA}^2/\text{molecule}$ for low laser power.

Further compression of the layer results in spectra (with better resolution) in the center panel, demonstrating that, although the CH_3 peaks grow in intensity, the CH_2 intensity remains constant up to the fully compressed monolayer, where it rapidly drops off. At the LE-LC transition at $A = 80 \text{ \AA}^2/\text{molecule}$, observed with fluorescence microscopy, no dramatic changes are observed in the VSGF spectra. This is not surprising since the surface changes at this transition are very slight. The results are summarized in the lower panel of Fig. 3: With increasing

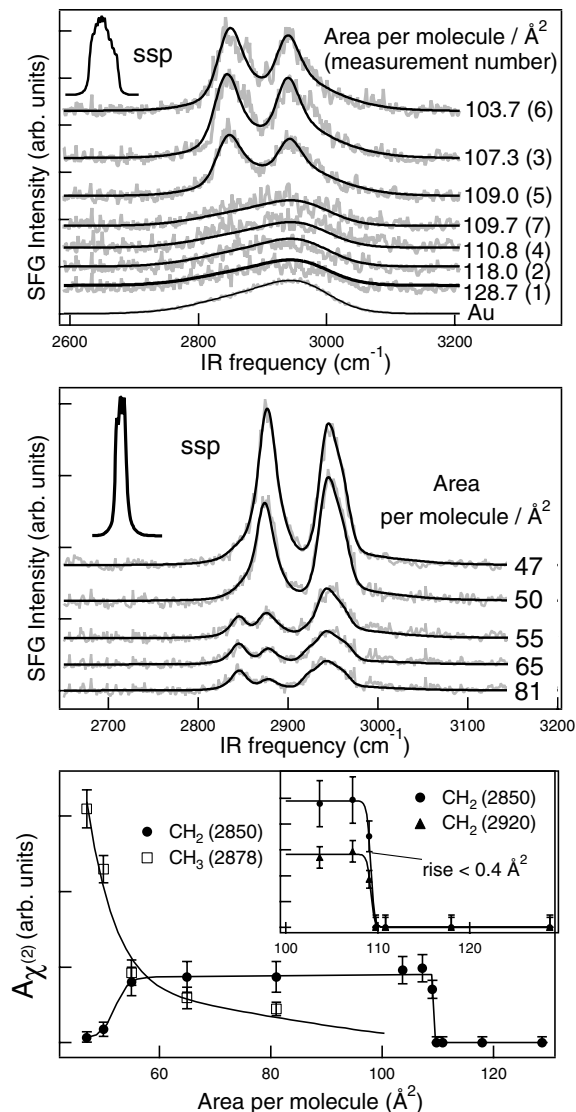


FIG. 3. Upper and middle panels: VSGF spectra (gray lines) upon compression of the DPPC monolayer. The upper panel also depicts the VSGF signal from a gold surface, to demonstrate the nonresonant nature of the signal for $A > 109.0 \text{ \AA}^2/\text{molecule}$. Black lines are fits described in the text. The spectral profile of the VIS up-conversion pulse is depicted in the upper left corner of the two upper panels. Lower panel: Amplitudes for the nonlinear susceptibilities for different vibrations obtained from the fits shown in the upper panels. Absolute values for the area per molecule may vary by 7%, but the relative values on the x axis are reliable within 0.5%. Lines in this panel are guides to the eye. The inset shows enlargement around the transition.

surface area, the amplitude of the CH_3 symmetric stretch ($\nu = 2878 \text{ cm}^{-1}$) decreases much more strongly than expected from the number of molecules, due to rapid onset of disorder: The signal is largest when all the dipoles are aligned. In contrast, for the CH_2 symmetric stretch ($\nu = 2850 \text{ cm}^{-1}$), the amplitude rises steeply with surface area due to the onset of disorder to level off at $55 \text{ \AA}^2/\text{molecule}$,

and remain at this value until the signal abruptly disappears at $109 \text{ \AA}^2/\text{molecule}$. The plateau can be understood by noting that the magnitude of this signal is determined by a competition between the number of CH_2 groups at the surface and the order in the alkyl chain: As their density increases (causing a larger signal), the chain-chain interactions also become more dominant, increasing the amount of order (resulting in a smaller signal, see above). Apparently, in the range $55\text{--}110 \text{ \AA}^2/\text{molecule}$, these two effects are in quite precise balance. Surprisingly, for $A > 110 \text{ \AA}^2/\text{molecule}$, the signal abruptly disappears indicating the alkyl chains become extremely disordered and regain inversion symmetry.

This anomalous behavior—the disappearance of VSFSG signal for constant surface coverage of alkyl chains—has been observed previously for a surfactant adsorbed to quartz [11], at a coverage identical to where the transition is observed here: at twice the surface area relative to fully compressed. In these experiments [11], the surface was in contact with solvents of varying polarity. As apolar solvent molecules interact with the alkyl chains, chain-chain interactions are increased, causing a lengthening and straightening out of the alkyl chains. In contrast, polar solvents were observed to cause a curling up of the chains, due to repulsive solvent-chain interactions; by curling up, the apolar alkyl chain can reduce its exposure to the polar environment, resulting in the disappearance of the VSFSG signal. In the case of DPPC, the relative strength of the water-chain interactions is increased as the coverage is decreased, and, apparently, there is a very clear point where the chain-water interactions supersede the chain-chain interactions, resulting in a sudden, conjunct coiling of the chains. As can be observed in the inset of Fig. 3 (lower panel), the width of the transition is less than $0.4 \text{ \AA}^2/\text{molecule}$ (the fitted line results in a width of $0.2 \text{ \AA}^2/\text{molecule}$). The narrow range over which the transition occurs can be understood by noting that, if for one chain (i.e., locally) the chain-water interactions exceed the chain-chain interactions and this chain curls up, its neighbor will experience less chain-chain interactions, causing it to curl up as well. As a result of this avalanche process, the transition is very sharp. As such, the observed transition cannot be the LE-G transition, which is known to exhibit a very large coexistence region. In contrast to fluorescence microscopy, VSFSG is insensitive to first order phase transitions with coexistence regions, such as the LE-G and the LE-LC transition, since the onset of coexistence initially affects only a small fraction of the molecules (and VSFSG is a majority probe, as is clear from the lower panel of Fig. 3). Inversely, as the molecular transition observed here with VSFSG does not result in mesoscopic changes

like domain formation, it remains undetected using fluorescence microscopy.

Previous observations of a sudden change in the non-linear response of Langmuir films in second harmonic generation (SHG) studies [12], as well as the otherwise typical behavior of DPPC as a surfactant [2], indicate that our observation of a molecular coiled-uncoiled transition is relevant to a wider range of systems.

The authors thank R. C. V. van Schie and P. Schakel for excellent technical support, and W. Roeterdink, D. Bonn, and A. W. Kleyn for many helpful discussions. This work is part of the research program of the Foundation for Fundamental Research on Matter (FOM), which is financially supported by the Netherlands Organisation for Scientific Research (NWO).

*Email address: m.bonn@chem.leidenuniv.nl

†Present address: Interfaculty Reactor Institute, Delft University of Technology, Mekelweg 15, 2629 JB Delft, Netherlands.

- [1] C. W. McConlogue and T. K. Vanderlick, *Langmuir* **13**, 7158 (1997); S. A. Kane, M. Compton, and N. Wilder, *ibid.* **16**, 8447 (2000).
- [2] V. M. Kaganer, H. Möwald, and P. Dutta, *Rev. Mod. Phys.* **71**, 779 (1999).
- [3] Y. R. Shen, *Nature (London)* **337**, 519 (1989), and references therein.
- [4] J. S. Salafsky and K. B. Eisenthal, *Chem. Phys. Lett.* **319**, 435 (2000).
- [5] R. A. Walker, J. C. Conboy, and G. L. Richmond, *Langmuir* **13**, 3070 (1997); R. A. Walker, J. A. Gruetzmacher, and G. L. Richmond, *J. Am. Chem. Soc.* **120**, 6991 (1998); J. Löbau, M. Sass, W. Pohle, C. Selle, M. H. J. Koch, and K. Wolfrum, *J. Mol. Struct.* **480–481**, 407 (1999).
- [6] T. Petralli-Mallow, K. A. Briggman, L. J. Richter, J. C. Stephenson, and A. L. Plant, *Proc. SPIE* **3858**, 25 (1999).
- [7] L. J. Richter, T. P. Petralli-Mallow, and J. C. Stephenson, *Opt. Lett.* **23**, 1594 (1998).
- [8] X. Zhuang, P. B. Miranda, D. Kim, and Y. R. Shen, *Phys. Rev. B* **59**, 12 632 (1999).
- [9] J. H. Hunt, P. Guyot-Sionnest, and Y. R. Shen, *Chem. Phys. Lett.* **133**, 189 (1987); Ch. Hess, M. Bonn, S. Funk, and M. Wolf, *ibid.* **325**, 139 (2000).
- [10] P. Guyot-Sionnest, J. H. Hunt, and Y. R. Shen, *Phys. Rev. Lett.* **59**, 1597 (1987).
- [11] P. B. Miranda, V. Pflumio, H. Saijo, and Y. R. Shen, *Chem. Phys. Lett.* **264**, 387 (1997); *J. Am. Chem. Soc.* **120**, 12 092 (1998).
- [12] Th. Rasing, T. Stehlin, Y. R. Shen, M. W. Kim, and P. Valint, Jr., *J. Chem. Phys.* **89**, 3386 (1988); Th. Enderle, A. J. Meixner, and I. Zschokke-Gränacher, *ibid.* **101**, 4365 (1994); A. Tojima, T. Manaka, and M. Iwamoto, *ibid.* **115**, 9010 (2001).